Highly-Efficient Holmium-Doped All-Fiber ~2.07-µm Laser Pumped by Ytterbium-doped Fiber Laser at ~1.13 µm

Alexander V. Kir'yanov, *Member, IEEE*, Yuri O. Barmenkov, *Member, IEEE*, Irma L. Villegas-Garcia, Jose L. Cruz, and Miguel V. Andres, *Member, IEEE*

***Abstract*—We report a 2.07-µm Holmium-doped all-fiber laser (HDFL) pumped by a 1.13-µm Ytterbium-doped fiber laser (YDFL). Home-made alumino-germano-silicate holmium-doped fiber (HDF) served here as active medium, optimized in terms of chemical composition and co-dopants' concentrations. Laser action at 2.07 µm was assessed in simple Fabry–Perot cavity, formed by a couple of home-made fiber Bragg gratings (FBGs), inscribed directly in the HDF; this allowed notable diminishing of intracavity loss of the 2.07-µm laser. HDF was in-core pumped by the 1.13-µm double-clad YDFL with power of ~12.5 W, in turn pumped in-clad by a laser diode (LD) operated at 0.97 µm with ~24.5-W output. Using optimal length (~5.0…5.5 m) of the HDF and employing FBG couplers with reflections of ~99% and ~33%, the HDFL provided ~5.0-W output at 2.07 µm. At these conditions, maximal absolute (slope) efficiencies at 2.07 µm of 39% (42%) and 20% (22%) were measured with respect to 1.13-µm (YDFL) and 0.97-µm (LD) pumps, respectively. Moreover, the record slope efficiency (48%) was obtained for the powers ratio of 2.07-µm output (HDFL) to launched 1.13-µm input (YDFL), which is only slightly less than theoretical quantum efficiency limit (53%) for this kind of pump schemes.**

***Index Terms*—Optical fiber lasers, Holmium**

I. Introduction

In the recent decade, considerable progress has been reached in development of 2-µm fiber sources, among which Holmium-doped fiber lasers (HDFLs) present special interest as capable of lase beyond 2 µm, in difference to Thulium-doped fiber lasers (TDFLs) that have a limit of operation wavelengths of around 2 µm. For HDFLs, the spectral domain 2.05…2.15 µm is currently well-explored [1-33], where researches have been mainly focusing on maximizing output power at continuous-wave (CW) lasing, accomplishing pulsed operations of different kind, and searching for some special oscillation regimes such as dual-wavelength lasing, soliton-supported lasing, etc.

Note that majority of to-date reported 2-µm HDFLs were laser-pumped, using mainly TDFLs with operation wavelengths 1.95…2.0 µm (to pump Ho^{3+} ions through $^5I_8\rightarrow{}^5I_7$ transition) or Ytterbium-doped fiber lasers (YDFLs) with operation wavelengths 1.12…1.15 µm (to pump Ho^{3+} ions through $^5I_8\rightarrow{}^5I_6$ transition). In the meantime, a few HDFL schemes were realized to-date at direct laser-diode (LD) pumping, also at 1.12…1.15 µm [8,33]. Apart of these methods to excite Ho^{3+} ions to get >2-µm lasing in 'pure' HDFs, such multielement systems as Ytterbium-Holmium and Thulium-Holmium silica fibers (YHDFs / THDFs), where Yb^{3+} or Tm^{3+} ions play the role of sensitizer, were demonstrated as effective for >2-µm lasing [1,5-7,19,20,23,24]. At using YHDFs / THDFs, energy transfer from the properly excited Yb^{3+} (Tm^{3+}) subsystem allows creating population inversion in the Ho^{3+} one, with subsequent release of excitation as lase beyond 2 µm, via Ho^{3+} transition $^5I_7\rightarrow{}^5I_8$.

Below, we present the results of our new study aiming to get effective, but simple in implementation, solution for a ~2-µm HDFL in-core pumped into $^5I_8\rightarrow{}^5I_6$ by an YDFL, in turn pumped in-clad by a moderate-power (25-W) LD operated @0.97 µm. Note that the basic components of this HDFL, viz., HDF of a new type and FBG-couplers, were home-made but can be easily reproduced elsewhere. We believe that success of the idea presented herein would deserve attention of specialists working in the area.

II. HDF's Characterization

The home-made HDF was drawn from the preform made employing the SPCVD technique (no solution-doping). The preform's core, apart from doping with Ho, was co-doped with Al, Ge, and F. In Fig. 1, we provide the data on material and waveguide properties of the preform: the radial distributions of (a) dopants' contents (in at. %) and (b) refractive-index (RI)

This work was supported in part by the Consejo Nacional de Ciencia y Tecnologia, Mexico, under Grant 242221 and in part by the Increase Competitiveness Program of NUST «MISIS» of the Ministry of Education and Science of the Russian Federation under Grant K3-2017-015. The work of A. V. Kir'yanov, Y. O. Barmenkov, and I. L. Villegas Garcia was supported by the Centro de Investigaciones en Optica, Leon, Mexico, through Internal Project "2 microns." The work of J. L. Cruz and M. V. Andres was supported by the Agencia Estatal de Investigación of Spain and Fondo Europeo de Desarrollo Regional (Ref.: TEC2016–76664-C2-1-R).

A. V. Kir'yanov is with the Centro de Investigaciones en Optica, Leon 37150, Mexico (phone: 52-477-441-4200; fax: 52-477-441-4209; e-mail: kiryanov@cio.mx) and the National University of Science and Technology (MISIS), Leninsky Avenue 4, Moscow 119049, Russia.

Y. O. Barmenkov is with the Centro de Investigaciones en Optica, Leon 37150, Mexico (e-mail: yuri@cio.mx).

I. L. Villegas Garcia is with the Centro de Investigaciones en Optica, Leon 37150, Mexico (e-mail: irlovg@cio.mx).

J. L. Cruz and M. V. Andres are with the Departamento de Fisica Aplicada, Instituto de Ciencia de Materiales, Universidad de Valencia, 46100 Valencia, Spain (e-mails: jose.l.cruz@uv.es; miguel.andres@uv.es).

Δn. The distributions of chemical elements constituting core-glass of the preform were obtained by means of electron-probe micro-analysis (EPMA), using an electron-ion microscope *FEI Quanta 3D FEG*. Note that Al and Ge were embedded into the preform's core-glass for engineering Δn and (Al) also for diminishing Ho^{3+} ions' clustering, whereas F was added for diminishing scattering at the core / cladding interface. In turn, the distribution of Δn was measured employing a RI preform analyzer (*Photon Kinetics A2600*). Note that the RI-difference in the preform was subject of preliminary optimization, by finding proper relations between Ho, Al, and Ge concentrations to provide the numerical aperture (NA) and core diameter of the final fiber compatible with those of an YDFL pump laser output (built using a commercial double-clad YDF, but see below its parameters).

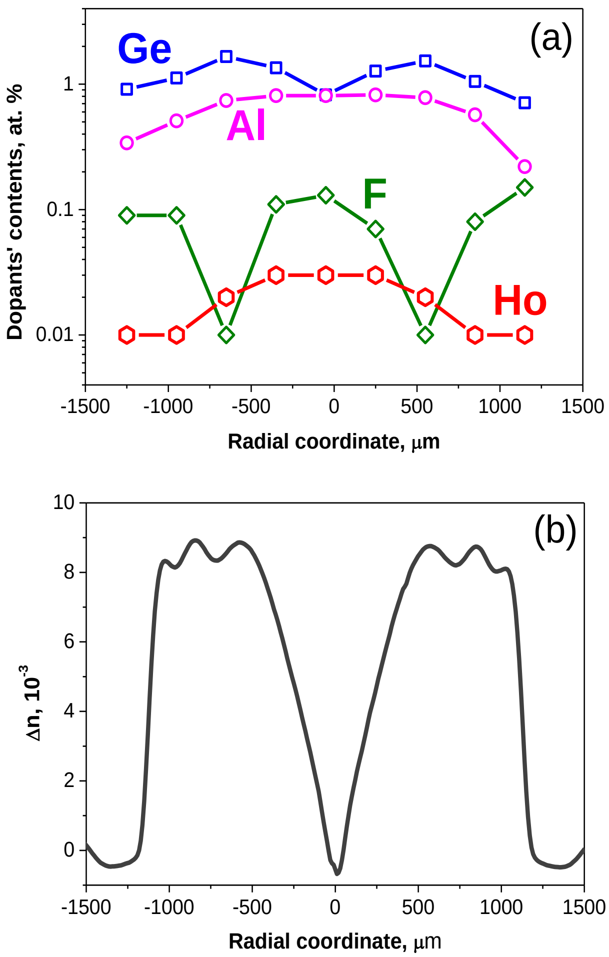

Fig. 1. (a) Radial distributions of dopants forming the HDF preform's core-glass: Ge (blue), Al (magenta), F (olive) and Ho (red); (b) radial distribution (black) of Δn in the preform's core area.

The radial distribution of absorption in the powerful peak of Ho^{3+} ions @452 nm is demonstrated in Fig. 2 (see inset). This result was obtained by measuring transmission of a thin (~0.6 mm) preform slice at white-light (WL) illumination (using *MOPS* equipment), at translating it along radius. In turn, the absorption spectrum collected from the central part of preform's core is exemplified in main area of Fig. 2.

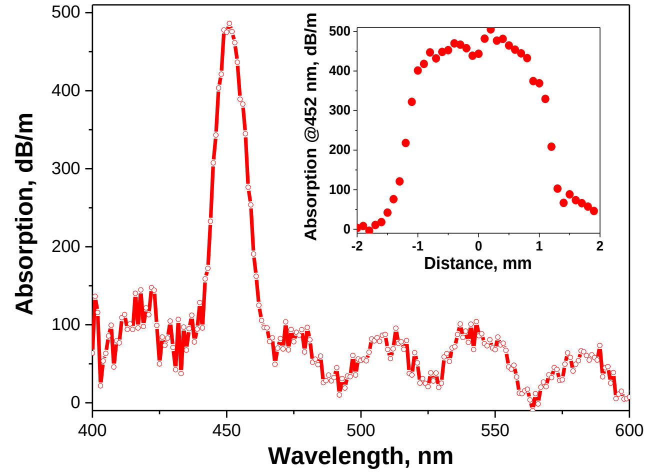

Fig. 2. (main area) Absorption spectrum in VIS of a slice cut-off from the HDF preform (the band peaking at 452 nm corresponds to Ho^{3+} transition $^5I_8 \rightarrow {}^5F_4$). (inset) Radial distribution of absorption in this band (proportional to Ho^{3+} ions radial concentration).

The waveguide parameters of the HDF were found to be as follows: cladding/core diameters – 125.0/10.5 μm; cutoff wavelength – 1.95 μm; NA – 0.14.

In Fig. 3, we show the absorption spectrum of the HDF drawn from the preform, measured in VIS-to-mid-IR spectral region. The spectrum was obtained using two optical spectrum analyzers (OSAs): *Ando 6315A* and *Yokogawa AQ6370B*.

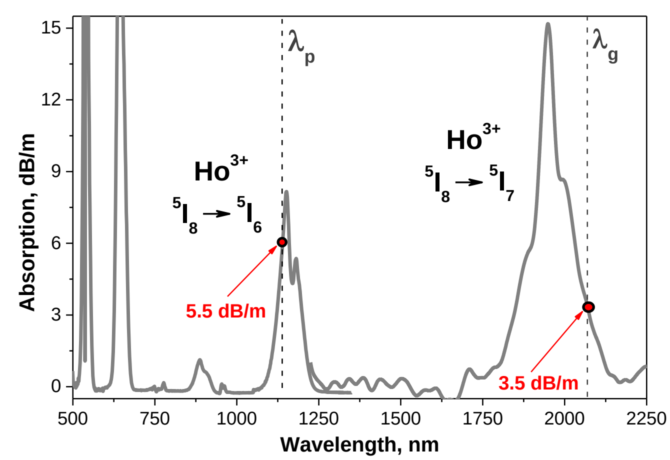

Fig. 3. Absorption spectrum of the HDF with the two Ho^{3+} bands ($^5I_8 \longrightarrow {}^5I_6$ and $^5I_8 \longrightarrow {}^5I_7$) relevant to laser experiments being indicated. Red arrows specify the absorption values at pump (λ_p) and generation (λ_p) wavelengths.

As seen from Fig. 3, the Ho^{3+} bands' structure is 'common' for HDFs: it is composed of the absorption bands peaking at ~1.15 μm in near-IR (transition $^5I_8 \rightarrow {}^5I_6$), ~1.95 μm in mid-IR (transition $^5I_8 \rightarrow {}^5I_7$), and a few bands in VIS. The near-IR/mid-IR absorption bands have peak values of ~8/~16 dB/m, respectively, whilst 'small-signal' absorption coefficients (α_0) within these two at the wavelengths chosen for pumping (λ_P= 1.13 μm) and lasing (λ_g= 2.07 μm) are measured by ~5.5 and ~3.5 dB/m, respectively (refer to the red arrows in the figure). The concentration of Ho^{3+} ions in the HDF is found from the absorption spectrum at assumption that absorption crosssection at 1.95 µm ($^5I_8 \rightarrow {}^5I_7$) is around $3 \cdot 10^{-21}$ cm^2 [17]), which gives an estimate of ~1.2×10^{19} cm^{-3}.

In Fig. 4, we demonstrate the data on fluorescent properties of the fiber. In inset, we provide the fluorescence spectrum of Ho^{3+} in mid-IR ($^5I_7 \rightarrow {}^5I_8$), obtained at ~1.13-µm excitation (0.5 W), while in the figure's main area we exemplify the kinetics (decay) of this fluorescence after switching-off (t=0) the pump light. The pump light was delivered from a commercial LD (*Innolume LD-1120HI-400*) and the fluorescence spectrum was measured using OSA *Yokogawa AQ6370B*. The mid-IR fluorescence (around 2 µm) was detected backward to pump-light, using a specialty wavelength-division multiplexor (WDM), passing both the pump and fluorescence lights (posteriorly, it was made a correction of the collected spectra, accounted for the WDM's spectral transmission). Pump-light at measuring fluorescence kinetics was switched on and off by biasing a rectangular modulation to the LD's driver at Hz-repetition rate; the launched pump power varied between zero and ~0.5 W. The fluorescence signal was detected using an InGaAs photo-detector (PD) (*Thorlabs DET10D*) with rise-time of 25 ns through a filter (*Thorlabs FEL-1550*), rejecting pump-light while transmitting light in the 2-µm range. The signals were collected on an oscilloscope (*Tektronix DPO7354C*). The overall setup's resolution was ~8 µs. Note that we experimented with short (tens cm) pieces of the HDF, for diminishing the effects of amplified spontaneous emission (ASE) and re-absorption on results.

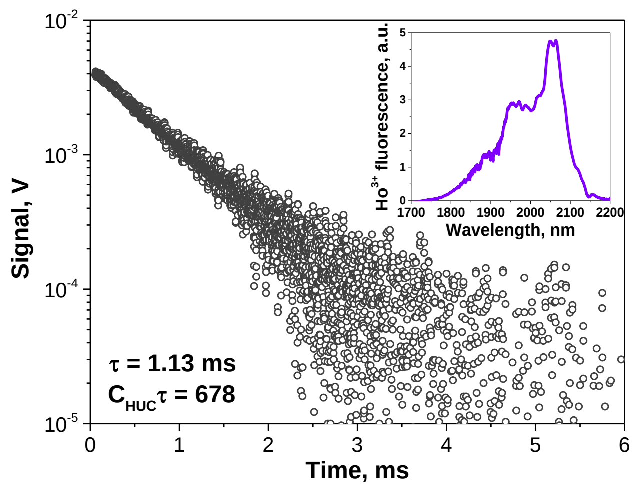

Fig. 4. (main area) ~2-µm ($^5I_7 \rightarrow {}^5I_8$) fluorescence decay at excitation at λ_p = 1.13 µm (via transition $^5I_8 \rightarrow {}^5I_6$); the values of fluorescence lifetime (τ) and its product with coefficient of homogeneous up-conversion (C_{HUC}) are indicated. (inset) Optical spectra of Ho^{3+} fluorescence in backward to pump light geometry. In both graphs, L_{HDF} = 3.0 m and pump power is 0.5 W.

As seen from Fig. 4, the mid-IR fluorescence covers a broadband spectral range, 1800…2200 nm, peaking at ~2.05 µm, while the fluorescence kinetic is very close to single exponent with decay time of τ=1.13 ms. [We used for fitting the experimental decay the method accounting for homogeneous up-conversion (HUC) between Ho^{3+} ions, attributed by coefficient C_{HUC} [34,35].] For this HDF, the product $C_{HUC}\tau$ was found to be 678; it is a quite small value, evidencing UC weakness in the fiber, favoring laser action at ~2 µm.

III. Results

The laser setup is sketched in Fig. 5 (top) and the scheme of Er^{3+} energy levels with the processes involved at ~2.07-µm lasing is presented in the figure's center. [In the figure's bottom, we provide the photo revealing lateral fluorescence in VIS of both the YDF and HDF at HDFL's lasing at the conditions of maximal pump power.]

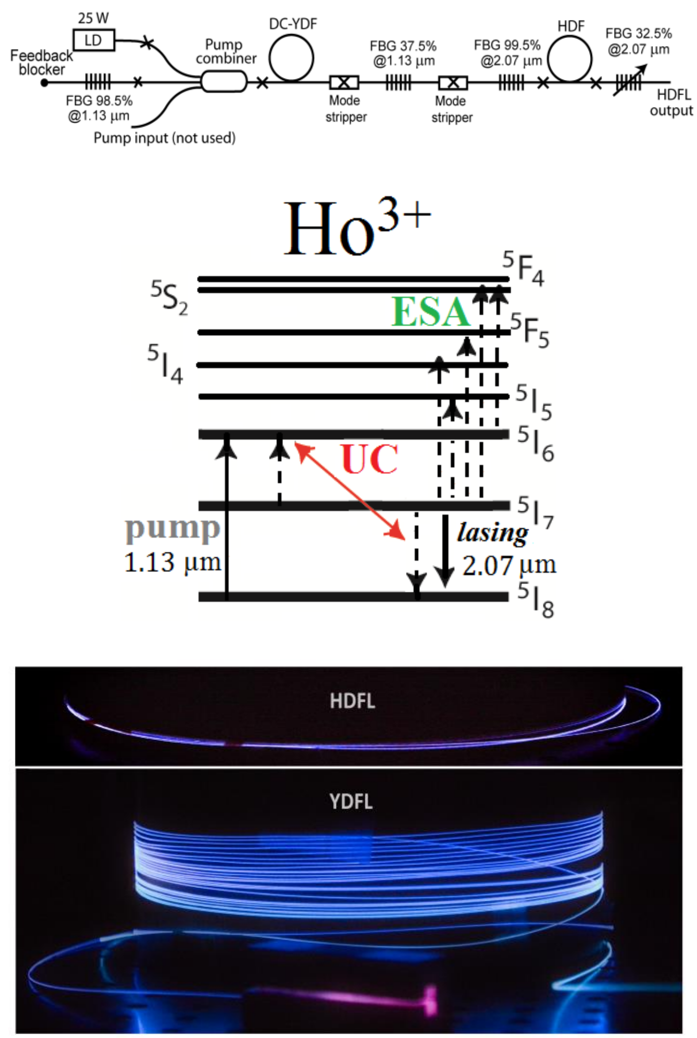

Fig. 5. (Top) Layout of the experimental setup (crosses mark splices); (center) schematics of Ho^{3+} levels along with the processes that may be involved at 1.13-µm pumping of HDF to get 2.07-µm lasing (HUC and ESA); (bottom) lateral view of the YDFL / HDFL system, operating in conditions of maximal pump power.

In experiments, a piece of the HDF was in-core pumped by an YDHL, built on the base of commercial double-clad (DC) YDF (SM-YDF-5/130-VIII from *Nufern*: core diameter, 5.5 µm, NA = 0.12, and cutoff @0.95 µm).

The YDFL cavity was composed of ~19 m of the YDF and two home-made FBGs ('rear' with reflectivity R=98.5% and 'output' with reflectivity R=37.5%), serving as cavity's couplers. The reflection spectra of these two FBGs are shown in Fig. 6.

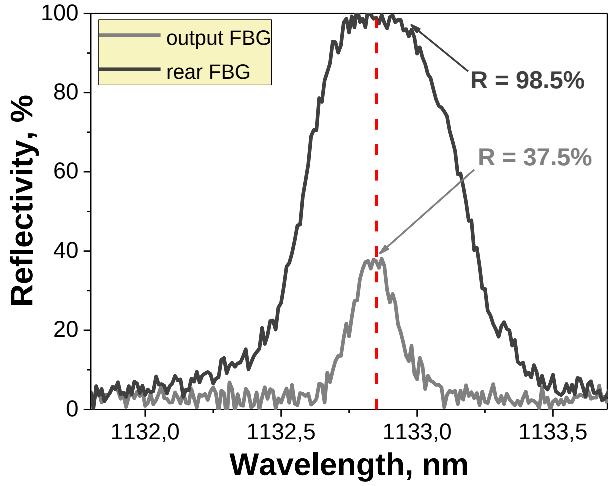

Fig. 6. Reflection spectra of the FBGs making-up the YDFL @1.13 µm.

As seen from Fig. 5(a), the DC-YDF was one-side pumped by a 0.97-µm LD (launched power, ~24.5 W) through a 2x1 combiner (but with only one input port being used at this stage of our work). Splicing of the YDF with the output FBG (R=37.5% @1.13 µm) was accomplished using a home-made silicon-filled mode stripper that removes the remnant (but small) portion of pump-light, not absorbed in the DC-YDF. On the other side of the YDFL, behind the rear FBG (R=98.5% @1.13 µm), another special silicon-filled unit was employed (a 'feedback blocker'), which provides strongly diminished Fresnel reflection from the end-cut of the fiber where this FBG was inscribed (otherwise, at the absence of such a unit, the YDFL might operate at 1.06...1.08 µm at high pump powers @0.97 µm).

Note here that all the clue parameters of the YDFL (YDF length, FBGs' reflectivity, etc.) have been subject of fine optimization prior to main-course experiments to ensure stable high-quality lasing @1.13 µm. The state-of-the-art of the YDFL's operation is presented in Figs. 7 and 8.

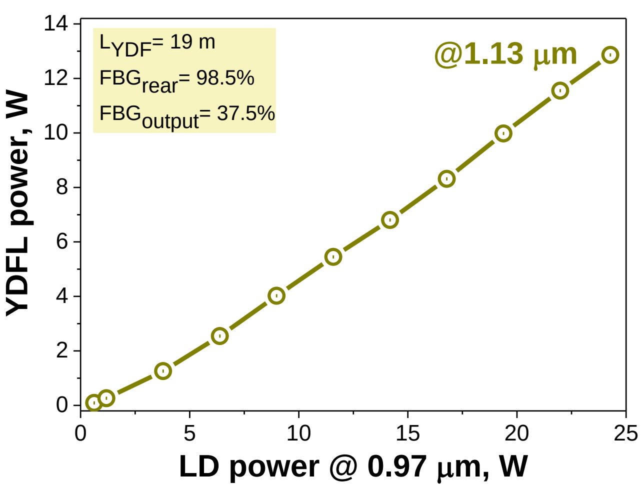

Fig. 7. Generation curves (1.13-µm output *vs.* LD pump power @0.97 µm); parameters of the laser are indicated in the inset.

In Fig. 7, we show the 'generation curve' of the YDFL, revealing that the laser provides output of up to ~12.5 W @1.13 µm (at maximal pump power delivered from the LD @ 0.97 µm: 24.5 W), at a quite low threshold (<0.5 W). In turn, Fig. 8 allows one to capture the spectral features of 1.13-µm lasing; particularly, it is seen (refer to main area of the figure) that no undesired lasing at 1.07…1.08 µm is developed in the system, even at the highest pumps delivered. In the meantime, it deserves noting that the spectral width of the laser line @1.13 µm considerably grows with increasing of output power (see inset).

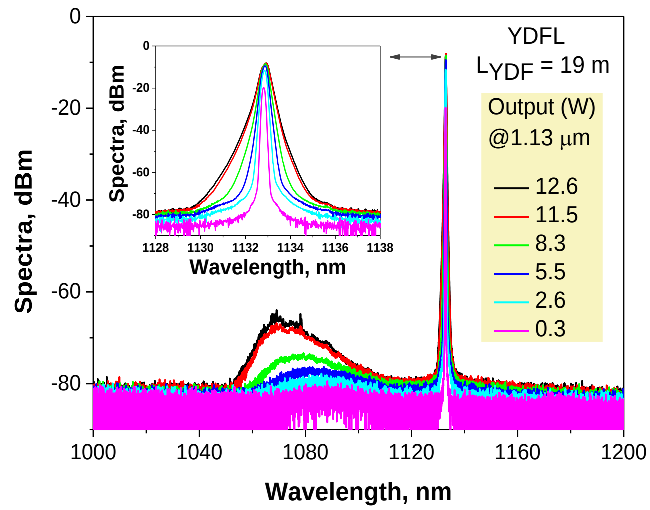

Fig. 8. (main area) Optical spectra at the YDFL output, specified for different laser powers; (inset) the same spectra zoomed, showing the laser line in detail.

The YDFL's output served as pump for the HDFL. As seen from Fig. 5(a), the pump light @1.13 µm was launched into the HDFL, formed by a piece of the HDF (variable in the experiments) and two FBGs @2.07 µm, through another silicon-filled mode stripper. This stripper served for removing, in a 'soft' regime, of a part (~13%) of pump light, not captured by the fiber where the rear FBG-coupler @2.07 µm – because of some inconsistency of the waveguiding parameters of this FBG (it was drawn in the active HDF) with the ones of the output FBG (@1.13 µm) of the pump YDFL. [Note here that the mentioned 13% loss of pump light, uncoupled to the HDF, was the main shortage, or 'weak chain', of our laser scheme, which ought to be decreased in future versions of the ~2-µm HDFL.]

The two home-made FBGs @2.07 µm (rear with reflectivity R=99.5% and output with reflectivity R=32.5%), served as cavity's couplers of the HDFL. The reflection spectra of these two FBG-couplers are shown in Fig. 9. It deserves emphasizing here that we inscribed the FBGs @2.07 µm directly in the active HDF (remind that this type of HDF co-doped with Ge has been specially fabricated to fit such opportunity) in order to diminish intracavity loss of the HDFL. However, because of heating of the gratings under the action of intracavity radiation (given by the presence of Ho), their reflection spectra slightly moved – at the high pump/laser powers – to Stokes side. This forced us to slightly tune the output FBG at increasing the pump power to compensate the effect of thermally-induced movement of the reflection spectra (mainly produced in the rear, highly-reflective, FBG @2.07

μm). This is schematically shown in Fig. 5(a) by the arrow in the output FBG @2.07 μm.

Also note that the Fabry-Perot cavity comprising these two FBGs was chosen to be of a relatively high Q-factor (we did not experiment with low output-coupler's reflection coefficients), permitting a low threshold. This was one of the critical requirements, given a notable (whereas unavoidable) Stokes-loss (~50%) owing to largely distant spectral positions of the pump and laser wavelengths in our circumstances, inherent to pumping via transition $^5I_8 \rightarrow ^5I_6$ of Ho^{3+}.

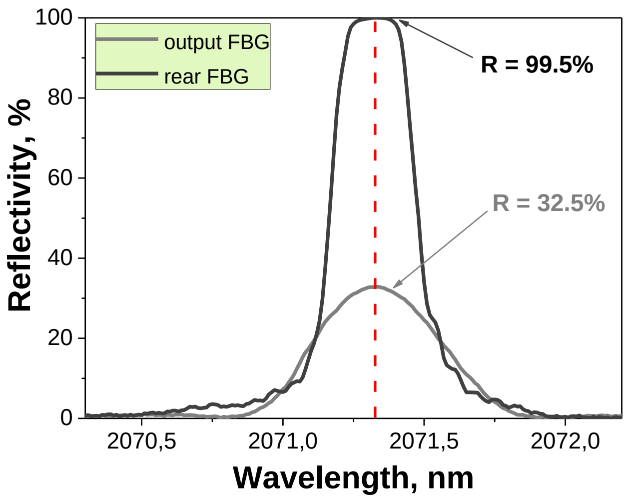

Fig. 9. Reflection spectra of the FBGs making-up the HDFL @2.07 μm.

The HDFL's parameters were measured employing the same equipment as described in Section II. In experiments, we varied only the pump power at 0.97 μm (LD) and HDF length. Note that in all cases featured below the HDFL lased in CW.

In Figs. 10-12, we provide the state-of-the art of the HDFL operation close to optimal (in the sense of HDF length: 5 to 6 m) conditions. In turn, in Figs. 13-15, we give a resume of the dependences of key characteristics of the laser in function of HDF length used.

The 'generation curve' of the HDFL built at the HDF with length of 5.3 m (see Fig. 10) reveals that the laser provides output of up to ~5.0 W @2.07 μm at maximal pump power delivered from the 0.97-μm LD (~24.5 W), which corresponds (compare with the 'generation curve' for the YDFL; refer to Fig. 7) to ~12.5 W @1.13 μm. That is, efficiency of the HDFL exceeds 20% (vs. 0.97-μm LD power) and 40% (vs. 1.13-μm YDFL power), correspondingly.

As far as we know, these are the highest to-date efficiencies, reported for a ~2-μm HDFL pumped via transition $^5I_8 \rightarrow ^5I_6$ of Ho^{3+}. Furthermore, notice a low threshold of the laser: threshold pump power is ~1.6 W @0.97 μm. As then seen from Fig. 11, the HDFL demonstrates a quite narrow (<0.3 nm) laser line, up to the highest pump/laser powers. The line's spectral form (but after adjustment applied to the output FBG @2.07 μm; see above) is almost symmetric. Despite the line 'moves' to the Stokes side (due to the mentioned thermal effect), its spectral form is kept almost unchanged within the whole pump range.

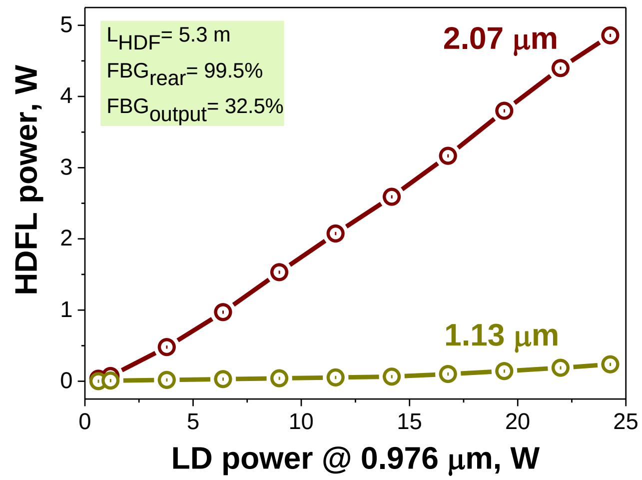

Fig. 10. Generation curves (2.07-μm output *vs.* LD pump power @0.97 μm); parameters of the laser are indicated in the inset.

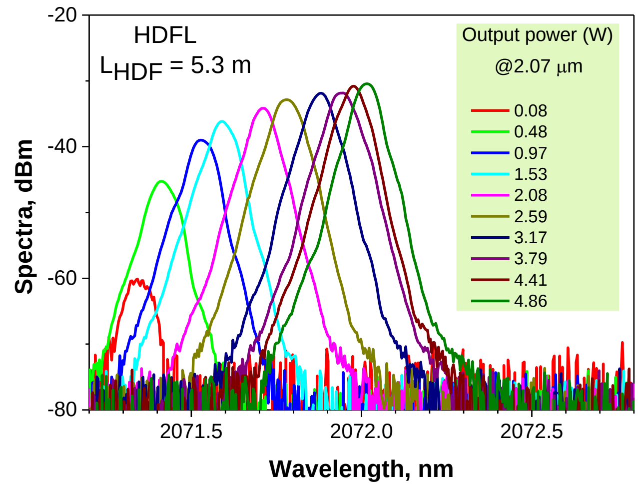

Fig. 11. Laser spectra at the HDFL output (L_{HDF} = 5.3 m), specified for different laser powers @2.07 μm.

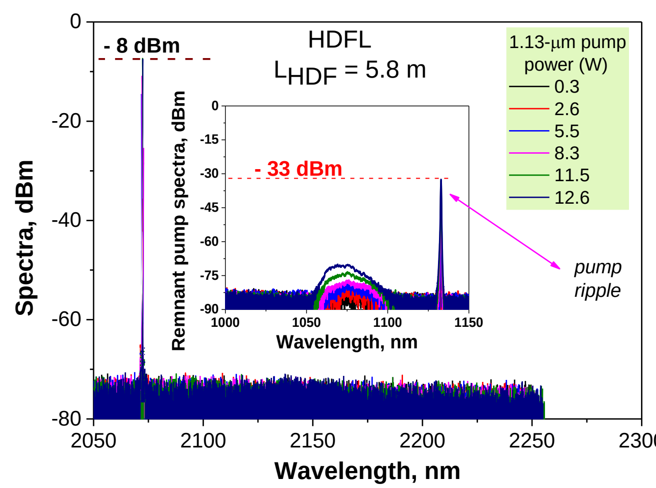

Fig. 12. (main area) Optical spectra at the HDFL output (L_{HDF} = 5.8 m), specified for different pump powers @1.13 μm; (inset) the spectra of remnant pump, measured at the same conditions.

As seen from Fig. 12, where we plot the optical spectra of the HDFL in a broader domain, lasing @2.07 mμ is almost free from 'contaminating' by the 1.13-μm pump remnants, in the whole range of pump powers launched: compare the magnitude of @2.07-mμ laser-line (-8 dBm in Fig. 12, corresponding to ~4.5 W, for HDF length of 5.8 m) with that of pump-light @1.13 mμ at the HDFL output (-33 dBm, corresponding to <200 mW).

In Figs. 13 and 14, we provide an overview of the HDFL's basic parameters, viz. (a) maximal 2.07-μm power at the output (left scale) and threshold pump power @0.97 μm delivered from the LD, and (b) remnant of ~1.13-μm power generated by the YDFL at the HDFL output.

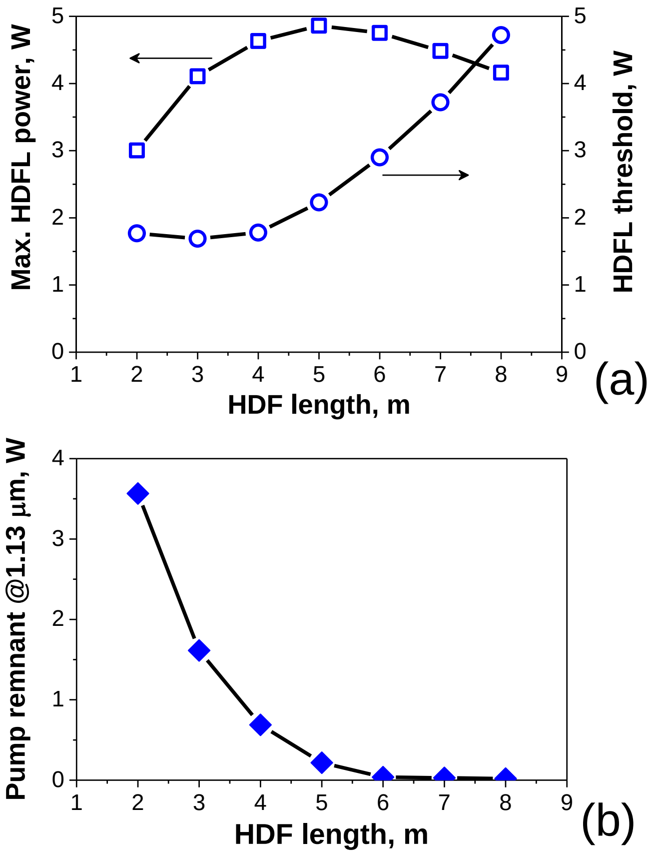

Fig. 13. Parameters of ~2.07-μm lasing *vs.* HDF length: (a) maximum laser power and threshold (LD) pump power @0.97 μm; (b) remnant (YDFL) pump power @1.13 μm *vs.* HDF length.

As seen from these figures, there are 'optimal' lengths of the HDF that build the HDFL, ranging from ~4.5 to ~5.6 m, for which maximal 2.07-μm powers (>4.7 W) at lowest 0.97-μm LD pump thresholds (<2.5 W) are releasable from the system while keeping minimal 'contaminating' by 1.13-μm (YDFL) light remnants (<300 mW). The found parameters' values of this HDFL's version lay a good guidance for further possible steps towards the current scheme's improvements, but, in general, they form its almost optimized state-of-the-art, given that (see below) the efficiency of 2.07-μm lasing is very close to the theoretical limit.

Indeed, as seen from Fig. 14, the absolute and slope efficiencies of the HDFL at 2.07 μm reach (at the HDF lengths varying around 5.0 m) 39% (42%) and 20% (22%) as measured with respect to 1.13-μm (YDFL: see the upper two curves in Fig. 14) and 0.97-μm (LD: see the lower two curves in Fig. 14) pump powers, respectively. To the best of our knowledges, the reported values of absolute/slope efficiencies of ~2-μm lasing are the best ones accessed to-date for HDFLs pumped into the 1.15-μm band of Ho^{3+}.

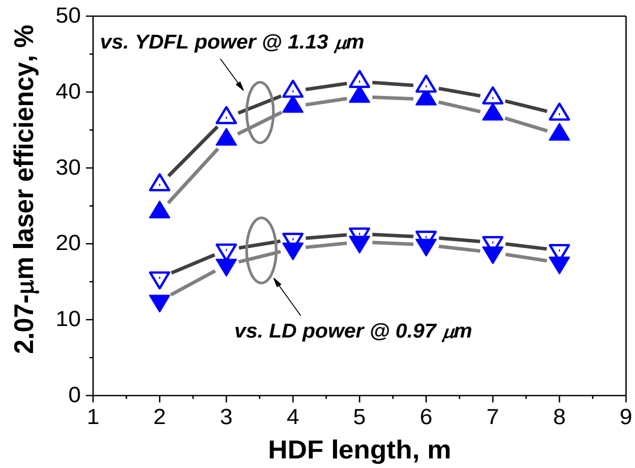

Fig. 14. Absolute (filled symbols) and slope (empty symbols) efficiencies of ~2.07-μm lasing *vs.* HDF length: upper two curves are obtained *vs.* the YDFL power @1.13 μm and lower two curves – *vs.* LD power @0.97 μm.

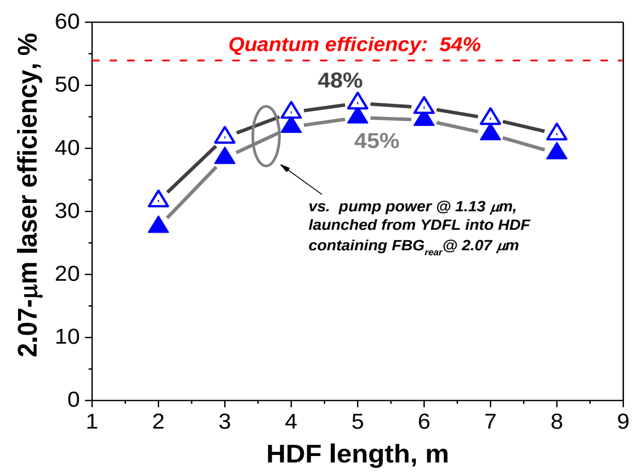

Fig. 15. Absolute (filled symbols) and slope (empty symbols) efficiencies of the HDFL at ~2.07 μm *vs.* HDF length with respect to pump power @1.13 μm, launched directly to the HDF with FBG_{rear} (@2.07 μm) drawn.

Moreover, see Fig. 15, the record slope/absolute efficiencies (~48%/~45%) have been measured by us for the powers' ratio of 2.07-μm output (the HDFL) to launched 1.13-μm input (the YDFL), which is only slightly less than the theoretical quantum efficiency limit (53%), inherent to this kind of pump schemes.

Emphasize that we don't pretend here that the HDFL, described above, demonstrates absolute power superior to the ones earlier reported for HDF-based laser systems at pumping via $^5I_8 \rightarrow ^5I_6$ band of Ho^{3+} ions. Say, a CW HDFL with output power as high as ~10 W (with over 30% slope efficiency) at ~2 μm was demonstrated at core-pumping, using an YDFL @1.15 μm [13]. However, this result has been obtained at the use of a couple of expensive high-power LDs with total output of ~70 W @0.975-nm for pumping that YDFL. We hypothesize that at making upgrade of our setup – by means of increasing the 0.97-μm pump power via adding one more LD to the pump port of the 2x1 combiner (see Fig. 5(a)) – it can be easily accessed ~2-μm lasing with >10 W of output power.

We believe that HDFLs, analogous to the one described above, may become broadly applicable for scientific researches and as master oscillators for power-scaling.

ACKNOWLEDGMENT

Authors are thankful for supporting this research work through the internal project '2 microns' by the Centro de Investigaciones en Optica (Leon, Mexico).

REFERENCES

[1] K. Oh, T.F. Morse, A. Kilian, et al., "Continuous-wave oscillation of thulium-sensitized holmium-doped silica fiber laser," *Opt. Lett.* 19, pp. 278-280, 1994.

[2] A.S. Kurkov, E.M. Dianov, O.I. Medvedkov, *et al.*, "Efficient silica-based Ho^{3+} fibre laser for 2 μm spectral region pumped at 1.15 μm," *Electron. Lett.*, vol. 36, pp. 1015–1016, 2000.

[3] M.J.F. Digonnet, ed. *Rare-earth doped fiber lasers and amplifiers*, (2nd edition), Marcel Dekker, New-York, pp. 4-10, 2001.

[4] S.D. Jackson, "2.7-W Ho^{3+}-doped silica fiber laser pumped at 1100 nm and operating at 2.1 μm," *Appl. Phys. B*, vol. 76, pp. 793-795, 2003.

[5] S. D. Jackson and S. Mossman, "Diode-cladding-pumped Yb^{3+}, Ho^{3+}-doped silica fiber laser operating at 2.1-μm," *Appl. Opt.*, vol. 42, pp. 3546-3549, 2003.

[6] S.D. Jackson and S. Mossman, "High-power diode-cladding-pumped Tm^{3+}, Ho^{3+}-doped silica fiber laser," *Appl. Phys. B*, vol. 77, pp. 489-491, 2003.

[7] S.D. Jackson, "Midinfrared holmium fiber lasers," *IEEE J. Quant. Electron.*, vol. 42, pp. 187-191, 2006.

[8] S.D. Jackson, F. Bugge, and G. Erbert, "Directly diode-pumped holmium fiber lasers," *Opt. Lett.*, vol. 32, pp. 2496-2498, 2007.

[9] S.D. Jackson, A. Sabella, A. Hemming, *et al.*, "High-power 83 W holmium-doped silica fiber laser operating with high beam quality," *Opt. Lett.*, vol. 32, pp. 241-243, 2007.

[10] A.S. Kurkov, E.M. Sholokhov, O.I. Medvedkov, *et al.*, "Holmium fiber laser based on the heavily doped active fiber," *Laser Phys. Lett.*, vol. 6, pp. 661-664, 2009.

[11] K.S. Wu, D. Ottaway, J. Munch, *et al.*, "Gain-switched holmium-doped fibre laser," *Opt. Express*, vol. 17, pp. 20872-20877, 2009.

[12] J.W. Kim, A. Boyland, J. K. Sahu, and W. A. Clarkson, "Ho-doped silica fibre laser in-band pumped by a Tm-doped fibre laser," in *Proc. Lasers Electro-Opt. Eur. Quantum Electron. Conf. (CLEO Europe - EQEC)*, 2009.

[13] A.S. Kurkov, V.V. Dvoyrin, and A.V. Marakulin, "All-fiber 10 W holmium lasers pumped at λ = 1.15 μm," *Opt. Lett.*, vol. 35, pp. 490-492, 2010.

[14] J. Geng, Q. Wang, T. Luo, *et al.*, "Single-frequency gain-switched Ho-doped fiber laser," *Opt. Lett.*, vol. 37, pp. 3795-3798, 2012.

[15] S. Hollitt, N. Simakov, A. Hemming, *et al.*, "A linearly polarized, pulsed Ho-doped fiber laser," *Opt. Express*, vol. 20, pp. 16285-16290, 2012.

[16] A. Hemming, S. Bennetts, N. Simakov, *et al.*, "High-power operation of cladding pumped holmium-doped silica fibre lasers," *Opt. Express*, vol. 21, pp. 4560-4566, 2013.

[17] N. Simakov, A. Hemming, W.A. Clarkson, *et al*., "A cladding-pumped tunable Holmium doped fiber laser," *Opt. Express*, vol. 21, pp. 28415-28422, 2013.

[18] E.J. Friebele, C.G. askins, J.R. Peele, et al., "Ho-doped fiber for high-energy laser applications," *Proc. SPIE*, vol. 8961, p. 896120-1, 2014.

[19] P. Honzatko, Y. Baravets, I. Kasik, and O. Podrazky, "Wideband Thulium-Holmium-doped fiber source with combined forward and backward amplified spontaneous emission at 1600-2300 nm spectral range," *Opt. Lett*., vol. 19, pp. 3650-3653, 2014.

[20] S. D. Jackson, "Towards high-power mid-infrared emission from a fibre laser", *Nature Photon.*, vol. 6, pp. 423-431, 2012.

[21] A.Yu. Chamorovskiy, A.V. Marakulin, A.S. Kurkov, *et al.*, "High-repetition-rate Q-switched Holmium fiber laser," *IEEE Photonics J.*, vol. 4, pp. 679-683, 2012.

[22] A. Chamorovskiy, A.V. Marakulin, S. Ranta, *et al.*, "Femtosecond mode-locked holmium fiber laser pumped by semiconductor disk laser," *Opt. Lett.*, vol. 37, pp. 1448-1451, 2012.

[23] A.V. Kir'yanov, V.P. Minkovich, and Y.O. Barmenkov, "All-fiber 2.05-μm continuous-wave Ytterbium–Holmium laser pumped at 1.064 μm,", *IEEE Phot. Tech. Lett.*, vol. 26, pp. 1924-1927, 2013.

[24] A.V. Kir'yanov, Y.O. Barmenkov, and V.P. Minkovich, "2.05-μm Ytterbium-Holmium doped all-fiber gain-switched pulsed laser pumped at 1064 nm," *Las. Phys. Lett.*, vol. 11, art. 126107, 2014.

[25] V. Dvoyrin, N. Tolstik, E. Sorokin, I. Sorokina, and A. Kurkov, "Graphene-mode-locked Holmium fiber laser operating beyond 2.1 μm," in *2015 European Conference on Lasers and Electro-Optics – European Quantum Electronics Conference*, 2015, paper CJ_7_4.

[26] C. Yao, C. He, Z. Jia, *et al*., "Holmium-doped fluorotellurite microstructured fibers for 2.1 μm lasing," *Opt. Lett.*, vol. 40, pp. 4695-4698, 2015.

[27] J. Albrecht, P. Peterka, P. Honzatko, *et al.*, "Self-swept Holmium-doped fiber laser near 2100 nm," in *Laser Congress 2016 (ASSL, LSC, LAC)*, 2015, paper JTu2A7.

[28] J. Sotor, M. Pawliszewska, G. Sobon, *et al.*, "All-fiber Ho-doped mode-locked oscillator based on a graphene saturable absorber," *Opt. Lett.*, vol. 47, pp. 2592-2595, 2016.

[29] J. Albrecht, P. Peterka, P. Honzatko, *et al.*, "Characterization of Holmium fibers with various concentrations for fiber laser applications around 2.1 μm," *Proc. SPIE*, vol. 9886, p. 988607, 2016.

[30] S.W.S. Ng, D.G. Lancaster, T.M. Monro, *et al*., "Air-clad Holmium-doped silica fiber laser," *IEEE J. Quant. Electron.*, vol. 52, art. 1600108, 2016.

[31] X. Jin, Z. Lou, Y. Chen., *et al*., "High-power dual-wavelength Ho-doped fiber laser at >2 μm tandem pumped by a 1.15 μm fiber laser," *Scientific Rep*., vol. 7, art. 42402, 2017.

[32] M. Hinkelmann, D. Wandt, U. Morgner, *et al*., "Mode-locked Ho-doped laser with subsequent diode-pumped amplifier in an all-fiber design operating at 2052 nm," *Opt. Express*, vol. 25, pp. 20522-20529, 2017.

[33] A.V. Kir'yanov, Y.O. Barmenkov, and I. Villegas Garcia, "2.05 μm holmium-doped all-fiber laser diode-pumped at 1.125 μm," *Laser Phys.*, vol. 27, art. 085101, 2017.

[34] A.V. Kir'yanov, Y.O. Barmenkov, G.E. Sandoval-Romero, and L. Escalante-Zarate, "Er^{3+} concentration effects in commercial Erbium-doped silica fibers fabricated through the MCVD and DND technologies," *IEEE J. Quant. Electron.*, vol. 49, pp. 511-520, 2013.

[35] A.V. Kir'yanov, V.V. Dvoyrin, V.M. Mashinsky, *et al*., "Nonsaturable absorption in alumino-silicate bismuth-doped fibers," *J. Appl. Phys.*, vol. 109, art. 023113, 2011.